Steady solutions of the Navier-Stokes equations by selective frequency damping

Espen Åkervik, Luca Brandt, Dan S. Henningson, Jérôme Hœpffner,
Olaf Marxen, and Philipp Schlatter[a)]
KTH Mechanics, SE-100 44 Stockholm, Sweden

A new method, enabling the computation of steady solutions of the Navier-Stokes equations in globally unstable configurations, is presented. We show that it is possible to reach a steady state by damping the unstable (temporal) frequencies. This is achieved by adding a dissipative relaxation term proportional to the high-frequency content of the velocity fluctuations. Results are presented for cavity-driven boundary-layer separation and a separation bubble induced by an external pressure gradient. © *2006 American Institute of Physics*. [DOI: 10.1063/1.2211705]

The knowledge of a steady base-flow solution of the governing Navier-Stokes equations is fundamental to instability studies and flow control. In the former case it allows for both linear modal and nonmodal analyses and weakly nonlinear approaches, whereas in the latter case the stabilization of such a base flow can be adopted as a design target. Recent developments, for example, as reviewed in Ref. 1 have allowed the research community to examine the stability of flows in increasingly complex configurations and to compute two- and three-dimensional eigenmodes, the so-called global modes.[2] Unfortunately, when the flow under consideration is globally unstable, it is virtually impossible to numerically compute a steady-state solution of the Navier-Stokes equations by time-marching methods, in particular for high-order schemes with inherently low numerical dissipation. In some limited cases solutions can be obtained by, e.g., artificially setting the velocity component in certain directions to zero or enforcing symmetries in the system, the most studied example for the latter case being the two-dimensional flow around a circular cylinder. For other cases, the only remaining possibility is the class of Newton iteration methods, which require heavy computational resources for large systems. In this article, we propose a simple numerical approach to compute steady solutions of the Navier-Stokes equations in unstable configurations. We show that it is possible to reach a steady state by damping the most dangerous frequencies and thus quenching the corresponding instability. The method is adapted from large-eddy simulation (LES) techniques, in particular the work of Pruett *et al.*[3,4]

Problem formulation: Consider the nonlinear system $\dot{q} = f(q)$, with appropriate initial and boundary conditions for the vector quantity q under the operator $f(q)$. (A dot is used here to denote the derivative with respect to time.) For a flow problem, the above system is the Navier-Stokes equation. A steady state q_s is then given by $\dot{q}_s = f(q_s) = 0$. If f is unstable, any $q \neq q_s$ will quickly depart from q_s. In order to stabilize the above system we propose applying regularization techniques common in control theory, in this case in the form of proportional (P) feedback control. This amounts to adding to

the right-hand side a linear term forcing towards a target solution w,

$$- \chi(q - w), \tag{1}$$

where χ is the control coefficient. The theoretical target solution for the control is of course the steady-state solution q_s, which is however not available *a priori*. Therefore, the actual target solution is a modification of q with *reduced temporal fluctuations*, i.e., a temporally low-pass filtered solution $w = T * q$, defined as the convolution of q with the temporal filter kernel T. For the method to converge asymptotically in time to an exact solution of the steady equation, the filter cutoff frequency should be lower than that of the flow instabilities. Therefore, in the following, the unstable frequency will be referred to as high frequency. With these definitions, the modified system is written as

$$\dot{q} = f(q) - \chi(I - T) * q, \tag{2}$$

where I is the identity operator. As q is approaching q_s, the filtered solution $w = T * q$ will in turn approach q, therefore reducing the control influence. If q is the actual steady solution, the time-filtered value w will be identical to $q = q_s$, yielding a vanishing forcing. Hence the steady solution q_s of the controlled system (2) is also a steady solution of the original problem. Note that there is no generation of new artificial steady states.

A related technique is also used in large-eddy simulation (LES) for the temporal approximate deconvolution model (TADM).[4] Working with spatial filters, a similar relaxation term has been successfully applied in the spectrally vanishing viscosity (SVV) concept[5] and in the (spatially filtered) approximate deconvolution model (ADM) (Ref. 6) and the ADM-RT model.[7] Following these modeling ideas, a different interpretation of the method can be given as follows. To attenuate unstable high-frequency temporal oscillations and thus reach a steady state we include in the momentum equations an additional linear regularization term, expression (1). This term is effectively damping the high-frequency content of q. Two parameters have to be chosen in the stabilization procedure, the filter shape T and the control gain χ. Time-domain filters are discussed first.
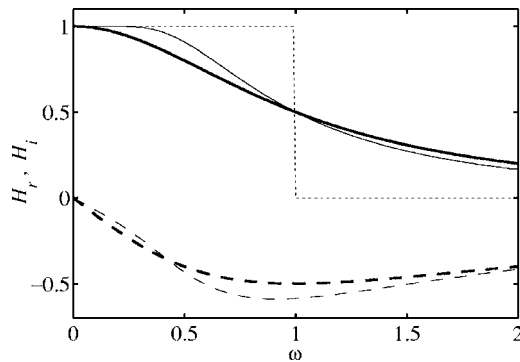

[a)]Electronic mail: pschlatt@mech.kth.se

FIG. 1. Real and imaginary part of the transfer function H of the exponential filter for degree $N=0$ and $N=4$, filter width $\Delta=1$. H_r^0 (thick solid); H_r^4 (thin solid); H_i^0 (thick dashed); H_i^4 (thin dashed); spectral (ideal) cutoff filter (dotted).

Time-domain filter: For a continuous function $q(t)$, a causal low-pass time filter is defined as

$$\bar{q}(t) = \int_{-\infty}^{t} T(\tau - t; \Delta)q(\tau)d\tau, \tag{3}$$

where $\bar{q}$ is the temporally filtered quantity, T is the parameterized filter kernel, and Δ is its associated filter width.[3] To be admissible, the kernel T must be positive and properly normalized. Additionally, in the limit of vanishing filter width the filter (3) must approach the Dirac delta function. Probably the simplest example of such a filter is the exponential kernel,

$$T(\tau - t; \Delta) = \frac{1}{\Delta} \exp\left(\frac{\tau - t}{\Delta}\right), \tag{4}$$

with the corresponding transfer function in the Fourier-Laplace space

$$H(\omega; \Delta) = \int_{-\infty}^{0} T(\tau; \Delta)\exp(i\omega\tau)d\tau = \frac{1}{1 + i\omega\Delta}, \tag{5}$$

where ω is the circular frequency and $i = \sqrt{-1}$. The cutoff frequency of the filter is defined as $\Re(H(\omega_c; \Delta)) = 1/2$ and is given by $\omega_c = 1/\Delta$. The transfer function of the filter is represented in Fig. 1 for a fixed filter width Δ. Note that the transfer function has a considerable imaginary part, which leads to a phase lag in the filtered signal relative to the original signal. For real applications, the integral formulation of the filter (3) is impractical, since it requires the storage of the complete time history of the signal q. Therefore, the equivalent differential form is adopted,

$$\dot{\bar{q}} = \frac{q - \bar{q}}{\Delta}, \tag{6}$$

which can be advanced in time using any integration scheme.

The order of the filter is defined as the index of the first nonvanishing derivative of $\Re(H(\omega))$ with respect to ω at $\omega = 0$, i.e., the filter (5) is of second order. Based on the exponential filter, also higher-order low-pass filters can be constructed by repeated application of the primary low-pass filter H.[4] The use of higher-order filters allows a better control over the separation between damped and undamped fre-

quencies. For specific cases, i.e., if the separation between instability mode and relevant flow phenomena is small, such a filter can be beneficial, e.g., in terms of convergence rate. Figure 1 displays the transfer function of the tenth-order filter (degree $N=4$, i.e. four applications of the exponential filter) with adapted filter width. This is one particular case of the general formulation where the shape of the filter transfer function can be tailored for specific demands.[8]

Stabilization of unstable steady solution: Analysis of the dynamics of the augmented system is presented in order to elucidate the stabilization procedure and quantify the effect of the control parameters. Considering system (2) with the exponential filter (6), i.e., $w = \bar{q}$, the system becomes

$$\left.\begin{array}{l} \dot{q} = f(q) - \chi(q - \bar{q}) \\ \dot{\bar{q}} = (q - \bar{q})/\Delta \end{array}\right\}. \tag{7}$$

The effect of the regularization can be illustrated by considering the eigenvalues of system (7) linearized about the steady state. Introducing the Jacobian A of f at the steady state q_s, the linearized system is

$$\begin{pmatrix} \dot{q} \\ \dot{\bar{q}} \end{pmatrix} = \begin{pmatrix} A - \chi I & \chi I \\ I/\Delta & -I/\Delta \end{pmatrix} \begin{pmatrix} q \\ \bar{q} \end{pmatrix}. \tag{8}$$

Assume $\mu = \mu_r + i\mu_i$ is a complex eigenvalue of A (i.e. $-i\mu\phi = A\phi$) with corresponding eigenvector ϕ. Observation of the structure of system (8) suggests that the eigenvectors of the new system will be $[\phi, \alpha\phi]^T$, where α is a complex number to be determined, and the corresponding eigenvalue will be $\lambda = \lambda(\mu, \alpha, \chi)$. Introducing this ansatz in (8), α and λ are obtained as

$$\alpha^{\pm} = \frac{-F \pm \sqrt{F^2 + 4\Delta\chi}}{2\Delta\chi}, \quad \text{with } F := \Delta(-i\mu - \chi) + 1,$$

$$\lambda^{\pm} = \mu - i\chi(1 - \alpha^{\pm}). \tag{9}$$

The two solutions α^+ and α^- give two eigenvalues λ^+ and λ^- for the modified system, originating from the same eigenvalue μ of the original system. The eigenvalue λ^+ can be seen as the damped original eigenmode, whereas λ^- is roughly associated with the filtering and corresponds to the $1/\Delta$ term in (8). The mapping $\mu \rightarrow \lambda^{\pm}$ in the complex plane is illustrated in Fig. 2 for parameters $\chi = 0.02$ and $\Delta = 15$. Two lines are represented (indicating possible eigenvalues μ of the original system), with imaginary parts 0.01 and -0.03, respectively. (These regions approximately correspond to the eigenvalues we are interested to damp in the cavity flow presented below.) Each line is mapped into two curves, the dashed one corresponding to λ^+, and the dashed-dotted line to λ^-. The arrows indicate how two points of the original solid lines are mapped into the new eigenvalues. It can be seen that points with large real part (corresponding to large circular frequency) are simply damped, i.e., shifted downwards, by a constant value χ, with virtually no shift along the real axis. Points of small real part are moved towards the origin exhibiting both a decrease in frequency and change in growth rate (imaginary part). The width of the hump forming at low frequencies is related to the filter cutoff frequency,
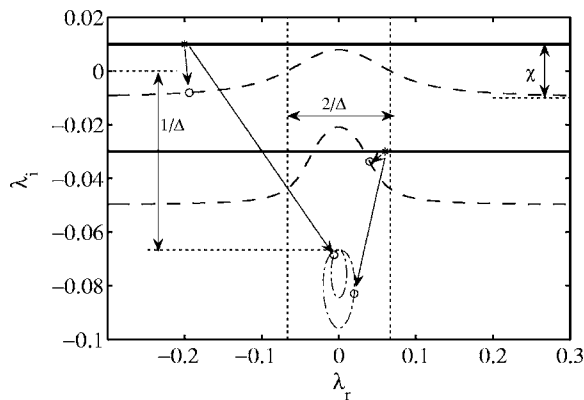
FIG. 2. Mapping of two lines ($\mu_i=0.01$ and $\mu_i=-0.03$, ——) in the complex plane due to the modified (linear) system (8). Two points originate from each complex eigenvalue μ, one point corresponding to λ^+ (---) and one corresponding to λ^- (-··-). $\chi=0.02$, $\omega_c=1/\Delta=1/15$.
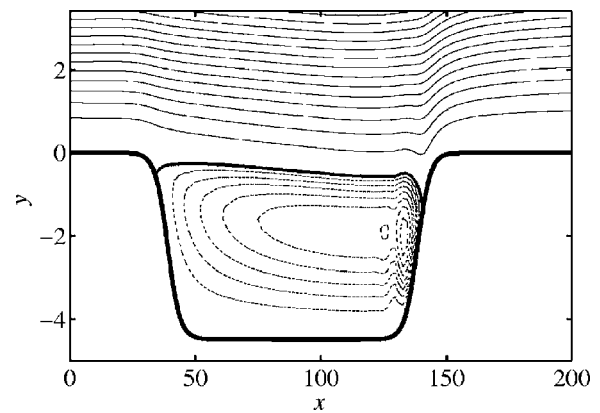

FIG. 3. Contour lines of the steady-state stream function for the cavity case. Zero stream function is indicated by the thick line, solid lines indicate positive values with spacing 0.2, dotted lines indicate negative values (spacing 0.025). The recirculation zone inside the cavity and the upward flow motion at the point of reattachment of the shear layer are clearly visible.

i.e., $1/\Delta$. It should be noted that a stable eigenvalue μ with low frequency will never be mapped into the unstable region.

In summary, the filter cutoff ω_c is related to the frequency of the relevant instabilities and should be smaller than those frequencies at which perturbation growth is expected. The gain χ is related to the growth rates of the instabilities and should be large enough to move the instability modes to the lower half plane. However, choosing a large χ will render the system evolution slow, since the low-frequency eigenvalues associated with the filter, λ^-, move towards the origin of the complex plane. The system will eventually converge to a steady state, but very slowly owing to the low damping rates. In order to have λ^+ as the least damped eigenvalue, χ needs to satisfy $\mu_i < \chi < \mu_i + 1/\Delta$. Similarly, when choosing a large Δ, the additional eigenvalues, whose imaginary parts cluster around $\omega_c = 1/\Delta$, will make the subsystem for $\bar{q}$ very slow. A balance has to be found for each system at hand to obtain quick convergence of all the time scales of the system. Testing several parameter pairs on the linear system (8) can be helpful. In cases where the Jacobian A cannot be approximated, like for the separation bubble presented below, the frequency of the instability can be estimated by considering the resulting unstable flow. As a guideline, the regularization parameter χ is chosen to be twice the growth rate of the dominant disturbance. The cutoff frequency, $\omega_c = 1/\Delta$ is chosen in such a way that the unstable disturbances are well within the damped region, e.g., $\omega_c \approx 1/2\omega_{\text{dist}}$. If the growth rate is unknown, one can estimate χ to be slightly smaller than $\mu_i + 1/\Delta \approx 1/\Delta$ assuming small μ_i.

Results: The selective frequency damping (SFD) method is applied to compute the steady state of the two-dimensional flow over a long cavity, and of the separation bubble induced by an external pressure distribution. Implementation of the present method into an existing code amounts to increasing the memory to store the filtered variable $\bar{q}$, adding the forcing term in the original time-marching scheme and advance the linear equation (6).

The stream function pertaining to the steady state of the cavity-driven separated flow is displayed in Fig. 3, where the streamwise and wall-normal coordinates are made nondi-

mensional with the inflow boundary-layer displacement thickness δ^*. The inflow profile is the Blasius profile at Reynolds number $\text{Re}_{\delta^*}=350$. This value has been chosen by gradually increasing it until a global unstable flow is obtained. The streamwise extent of the computational domain is $L_x=409$, with the cavity being confined to an area of $x \in [30, 150]$, whereas the wall-normal height is $L_y=80$. The numerical code uses fourth-order central finite differences and Chebyshev collocation in the streamwise and wall-normal direction, respectively. The time integration is carried out by a semi-implicit second-order backward Euler/Adams-Bashforth scheme.[9] Time history of the streamwise velocity measured just above the cavity is shown in Fig. 4 for two different simulations. In the first simulation, the SFD is active from the beginning of the computation where a zero initial condition is used, whereas in the second simulation SFD is switched on at time $t=3000$. Both simulations eventually converge to exactly the same steady state, in one case smoothly and in the other by damping the existing oscillations, the saturated unstable global mode.

In the case of the separation bubble, a flow field subject to a pressure gradient prescribed via the streamwise velocity at the upper boundary is computed. The equations are solved in vorticity-velocity formulation, with the relaxation term
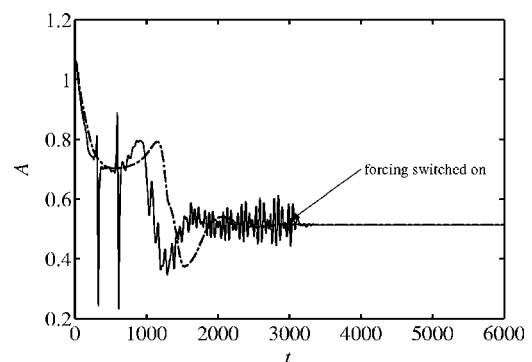

FIG. 4. Time history of streamwise velocity measured just above the cavity at $x=153.4$, $y=0.8485$. (—·—): Simulation started with zero initial condition. (——): SFD turned on at $t=3000$. Both cases are converging to identical steady states.
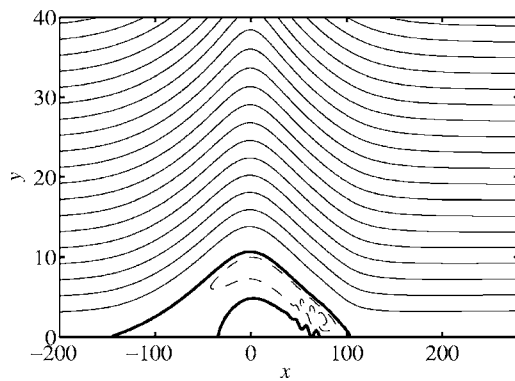
FIG. 5. Contour lines of the stream function for the separation bubble. Zero stream function is indicated by the thick line, solid lines indicate positive values with spacing 0.1, dashed lines indicate negative values (spacing 0.005).

$-\chi(\vartheta_z - \bar{\vartheta}_z)$ being added to the right-hand side of the transport equation for the spanwise vorticity ϑ_z. The code uses fourth/sixth-order finite differences on a Cartesian grid for the streamwise and wall-normal discretization together with an explicit fourth-order Runge-Kutta time integration.[10] For the present case, a Blasius profile is prescribed at the inflow ($\mathrm{Re}_{\delta^*}=1000$) while at the upper boundary, the streamwise velocity is quickly decreasing to about 10% of the free-stream velocity and then increases again. The box size is $L_x \times L_y = 562 \times 64$, and $\chi=0.4$, $\Delta=0.75$. Two different resolutions (801×193 and 1601×385) were used, with the time step adapted accordingly. The resulting steady state is shown in Fig. 5. To check convergence towards an exact solution of the steady equations, the absolute difference between the filtered and the unfiltered vorticity $\vartheta_z - \bar{\vartheta}_z$ was sampled over time and its maximum in the domain is plotted in Fig. 6. Without the SFD, no steady state could be reached. The damped oscillatory behavior visible in Fig. 6 is not related to the frequency of the vortex shedding. It is conjectured that this is an indication of a stable oscillatory movement of the bubble itself, i.e., so-called flapping of the separation bubble. Note that the quantity $\vartheta_z - \bar{\vartheta}_z$ displayed in Fig. 6 is in fact proportional to both the amplitude of the relaxation term and the time derivative of the evolution equation of the filtered

solution, $\bar{\vartheta}_z$. The simultaneous vanishing (to order 10^{-6}, which is sufficiently accurate for most applications) of $\partial\bar{\vartheta}_z/\partial t$ and the relaxation term as t becomes large implies that ϑ_z and $\bar{\vartheta}_z$ each essentially attain time independence; that is, a steady state has been achieved. Additionally, both grid resolutions showed the exact same convergence behavior which further stresses the point that an actual physical solution has been found. We also checked that no drifting of the steady solution is present by considering the evolution of $\vartheta_z(t+T) - \vartheta_z(t)$ over time t with T being large compared to the dominant shedding frequency. A similar behavior as in Fig. 6 was found and the diagram is therefore not shown here. In the case of the laminar separation bubble, the flow parameters are not incremented to follow a bifurcation but the pressure distribution is chosen arbitrarily to have an unstable flow. We thus show that the method allows attainment of a steady state without any initial guess. Of course, the initial condition becomes relevant in cases where multiple steady states coexist.

Conclusions: A simple numerical approach to compute steady solutions of the Navier-Stokes equations is presented. The most attractive advantages of such a strategy can be summarized as follows: It is easy to implement into an existing numerical code; it does not require a good initial guess of the solution; steady states can be computed without specific knowledge of the critical bifurcation parameters. To our experience, the SFD method appears to be very robust, and therefore this procedure provides a viable alternative to the classic Newton method.
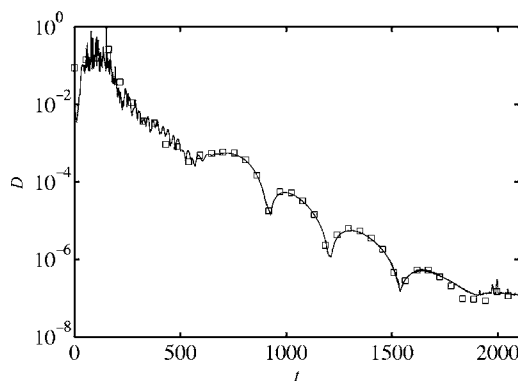
FIG. 6. Convergence towards steady state for the separation-bubble case, showing the maximum difference between the filtered and unfiltered vorticity field, $D=\max_{x,y}|\vartheta_z - \bar{\vartheta}_z|$.——, lower resolution; □, higher resolution.

[1] V. Theofilis, "Advances in global linear instability analysis of nonparallel and three-dimensional flows," Prog. Aerosp. Sci. **39**, 249 (2003).

[2] J.-M. Chomaz, "Global instabilities in spatially developing flows: Non-normality and nonlinearity," Annu. Rev. Fluid Mech. **37**, 357 (2005).

[3] C. D. Pruett, T. B. Gatski, C. E. Grosch, and W. D. Thacker, "The temporally filtered Navier-Stokes equations: Properties of the residual stress," Phys. Fluids **15**, 2127 (2003).

[4] C. D. Pruett, B. C. Thomas, C. E. Grosch, and T. B. Gatski, "A temporal approximate deconvolution model for large-eddy simulation," Phys. Fluids **18**, 028104 (2006).

[5] E. Tadmor, "Convergence of spectral methods for nonlinear conservation laws," SIAM (Soc. Ind. Appl. Math.) J. Numer. Anal. **26**, 30 (1989).

[6] S. Stolz, N. A. Adams, and L. Kleiser, "An approximate deconvolution model for large-eddy simulation with application to incompressible wall-bounded flows," Phys. Fluids **13**, 997 (2001).

[7] P. Schlatter, S. Stolz, and L. Kleiser, "LES of transitional flows using the approximate deconvolution model," Int. J. Heat Fluid Flow **25**, 549 (2004).

[8] T. Kailath, *Linear Systems* (Prentice-Hall, Upper Saddle River, 1980).

[9] M. Marquillie and U. Ehrenstein, "On the onset of nonlinear oscillations in a separating boundary-layer flow," J. Fluid Mech. **490**, 169 (2003).

[10] M. J. Kloker, "A robust high-resolution split-type compact FD scheme for spatial direct numerical simulation of boundary-layer transition," Appl. Sci. Res. **59**, 353 (1998).